Supporting Information

Heterometallic $\{Dy^{III}_2Fe^{II}_2\}$ Grids with Slow Magnetic Relaxation and Spin Crossover

Yu Zhang,[a] Qianqian Yang,[a,b] Jingjing Lu,[a] Mei Guo,[a] Xiao-Lei Li,[a] and Jinkui Tang*[a,b]

[a.]State Key Laboratory of Rare Earth Resource Utilization, Changchun Institute of Applied Chemistry, Chinese Academy of Sciences, Changchun, China.
E-mail: tang@ciac.ac.cn
[b.]University of Science and Technology of China, Hefei, China

Materials and general procedures

Unless otherwise noted, all chemical reagents and solvents used in this work were commercially acquired and used without any further purification. The elemental analyses were performed on a PerkinElmer 2400 analyzer. H NMR spectra were measured on a BRUKER 400M spectrometer. The fourier transform infrared (FTIR) spectra were recorded on a Nicolet 6700 Flex FTIR spectrometer equipped in the range from 500 to 4000 cm^{-1}. Magnetic susceptibility measurements were performed with a Quantum Design MPMS-XL7 SQUID device. The variable-temperature magnetization were measured using an external magnetic field of 1000 Oe and temperatures ranging from 1.9 to 375 K. The dynamics of the magnetization were investigated from the alternating-current (ac) measurements using a 3.0 Oe ac field oscillating and frequencies ranging from 1 to 1500 Hz. The diamagnetic corrections for all the constituent atoms were estimated with Pascal's constants and sample holder calibration.[1]

X-ray crystallography

Data collection and structure solution were performed using SMART and SAINT programs, respectively. All the structures were solved using direct methods with SHELXS and refined on F^2 by full-matrix least-squares using SHELXTL-2014 software package.[2,3] The locations of the heaviest atoms (Dy and Fe) were easily determined, and the other non-hydrogen atoms were refined anisotropically using full-matrix least-square procedures. All the hydrogen atoms were introduced in calculated positions and a riding model was used. Despite rapid handling times and a low-temperature collection, the quality of data was less than ideal. For all of the four data, the remaining solvent molecules or anions within the lattice were significantly disordered, which leads to a series of Alert level B in checkcif report. All the mean plane analyses as well as molecular drawings were obtained from DIAMOND (version 3.1). The information of coordination geometries were acquired by SHAPE analysis (Tables S4 and S11).[4-7] Details for the crystallographic information are summarized in Table 1, and selected bond distances and angles are exhibited in Tables S1-S2 and S4-9. CCDC 1996523-1996526 contains the supplementary crystallographic data for this paper. All the data can be obtained free of charge from the Cambridge Crystallographic Data Centre via https://www.ccdc.cam.ac.uk/structures.

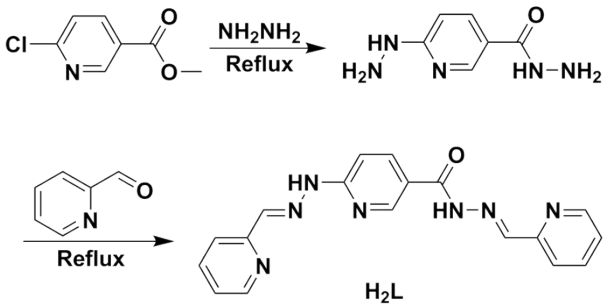

Figure S1. The synthetic routes of the H_2L.

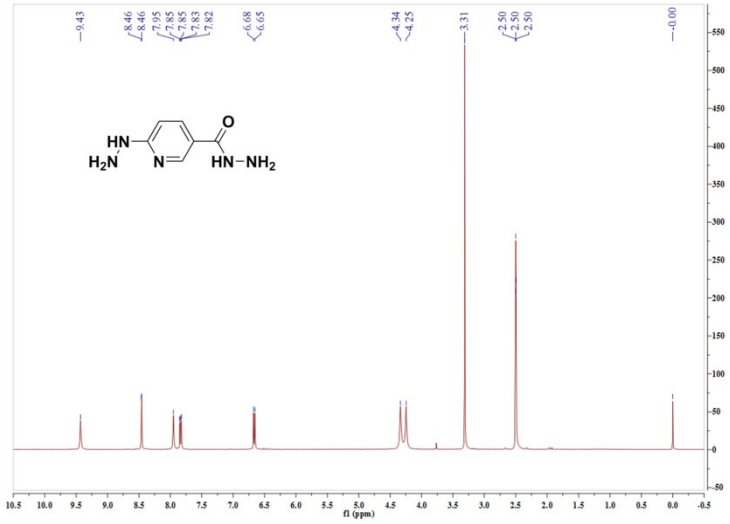

Figure S2. ^{1}H NMR spectra of 6-hydrazinylnicotinohydrazide.

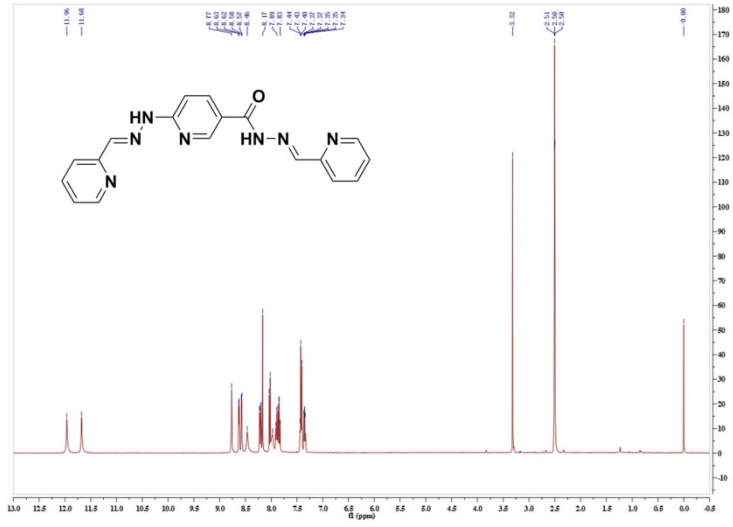

Figure S3. ^{1}H NMR spectra of H_2L.

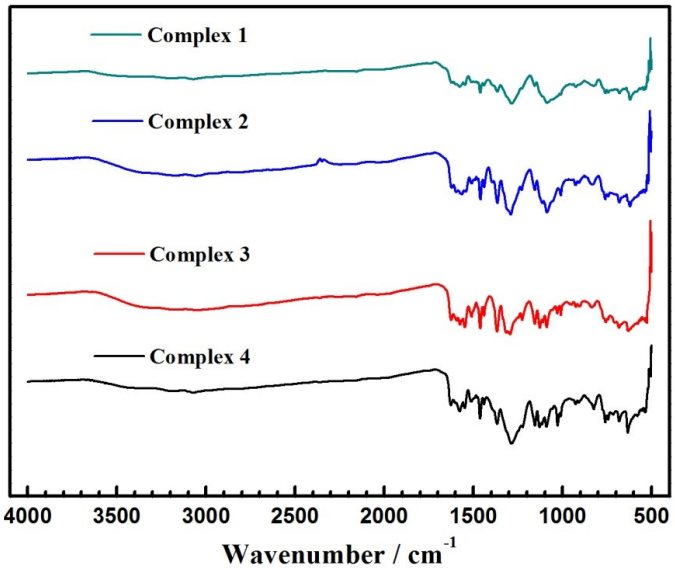

Figure S4. IR spectra of complexes **1**-**4**.

Table S1. Selected bond lengths (Å) for complex **1**.

Atom-Atom	Length/Å	Atom-Atom	Length/Å
Dy(1)-O(1)	2.386(5)	Dy(1)-N(1)	2.575(8)
Dy(1)-O(2)	2.382(5)	Dy(1)-N(2)	2.535(7)
Dy(1)-O(3)	2.365(6)	Dy(1)-N(12)	2.603(7)
Dy(1)-O(4)	2.372(6)	Dy(1)-N(13)	2.508(7)
Dy(1)-O(5)	2.380(6)		
Fe(1)-N(4)	1.962(6)	Fe(1)-N(8)	1.959(6)
Fe(1)-N(6)	1.856(7)	Fe(1)-N(9)	1.836(7)
Fe(1)-N(7)	1.972(7)	Fe(1)-N(11)	1.984(6)

Symmetry transformations used to generate equivalent atoms: #1 -x+1, -y+1/2, z+0

Table S2. Selected bond angles (°) for complex **1**.

Atom-Atom-Atom	Angle/°	Atom-Atom-Atom	Angle/°
O(3)-Dy(1)-O(4)	70.8(2)	O(5)-Dy(1)-N(2)	72.4(2)
O(3)-Dy(1)-O(2)	73.3(2)	O(1)-Dy(1)-N(2)	62.56(19)
O(4)-Dy(1)-O(2)	139.4(2)	N(13)-Dy(1)-N(2)	113.4(2)
O(3)-Dy(1)-O(5)	143.1(2)	O(3)-Dy(1)-N(1)	81.6(2)
O(4)-Dy(1)-O(5)	72.3(2)	O(4)-Dy(1)-N(1)	76.4(2)
O(2)-Dy(1)-O(5)	139.4(2)	O(2)-Dy(1)-N(1)	80.1(2)
O(3)-Dy(1)-O(1)	138.9(2)	O(5)-Dy(1)-N(1)	87.9(2)
O(4)-Dy(1)-O(1)	139.74(19)	O(1)-Dy(1)-N(1)	125.0(2)
O(2)-Dy(1)-O(1)	80.79(19)	N(13)-Dy(1)-N(1)	140.1(2)
O(5)-Dy(1)-O(1)	74.8(2)	N(2)-Dy(1)-N(1)	62.4(2)
O(3)-Dy(1)-N(13)	72.8(2)	O(3)-Dy(1)-N(12)	92.5(2)
O(4)-Dy(1)-N(13)	120.8(2)	O(4)-Dy(1)-N(12)	74.1(2)
O(2)-Dy(1)-N(13)	63.66(19)	O(2)-Dy(1)-N(12)	126.2(2)
O(5)-Dy(1)-N(13)	130.5(2)	O(5)-Dy(1)-N(12)	79.5(2)
O(1)-Dy(1)-N(13)	67.2(2)	O(1)-Dy(1)-N(12)	77.6(2)
O(3)-Dy(1)-N(2)	130.1(2)	N(13)-Dy(1)-N(12)	62.6(2)
O(4)-Dy(1)-N(2)	125.7(2)	N(2)-Dy(1)-N(12)	135.7(2)
O(2)-Dy(1)-N(2)	67.66(18)	N(1)-Dy(1)-N(12)	150.2(3)
N(9)-Fe(1)-N(6)	179.8(3)	N(8)-Fe(1)-N(7)	93.2(2)
N(9)-Fe(1)-N(8)	79.7(3)	N(4)-Fe(1)-N(7)	161.4(3)
N(6)-Fe(1)-N(8)	100.5(3)	N(9)-Fe(1)-N(11)	81.6(3)
N(9)-Fe(1)-N(4)	99.5(3)	N(6)-Fe(1)-N(11)	98.2(3)
N(6)-Fe(1)-N(4)	80.5(3)	N(8)-Fe(1)-N(11)	161.3(3)
N(8)-Fe(1)-N(4)	89.6(2)	N(4)-Fe(1)-N(11)	93.7(3)
N(9)-Fe(1)-N(7)	99.2(3)	N(7)-Fe(1)-N(11)	89.6(3)
N(6)-Fe(1)-N(7)	80.9(3)		

Symmetry transformations used to generate equivalent atoms: #1 -x+1, -y+1/2, z+0

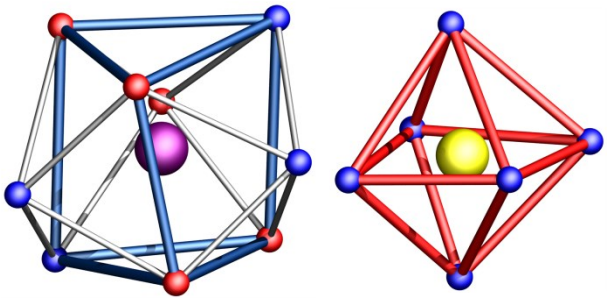

Figure S5. Coordination polyhedra observed in complex **1**: spherical tricapped trigonal prism for Dy1 (blue) and octahedral environment for Fe1 (red), respectively.

Table S3. Dy^{III} and Fe^{II} ions geometry analysis of complexes **1-3** by SHAPE 2.1 software.[4-7]

Complex **1**

	JTC (C_{3v})	JCCU (C_{4v})	CCU (C_{4v})	JCSAPR (C_{4v})	CSAPR (C_{4v})	JTCTPR (D_{3h})	TCTPR (D_{3h})
Dy(1)	14.915	10.250	8.240	2.083	1.348	2.280	1.097
	HP (D_{6h})	PPY (C_{5v})	OC (O_h)	TPR (D_{3h})	JPPY (C_{5v})		
Fe(1)	33.356	23.953	1.914	12.353	27.941		

Complex **2**

	JTC (C_{3v})	JCCU (C_{4v})	CCU (C_{4v})	JCSAPR (C_{4v})	CSAPR (C_{4v})	JTCTPR (D_{3h})	TCTPR (D_{3h})
Dy(1)	14.916	10.251	8.231	2.214	1.497	2.311	1.114
	HP (D_{6h})	PPY (C_{5v})	OC (O_h)	TPR (D_{3h})	JPPY (C_{5v})		
Fe(1)	34.280	24.128	2.015	12.534	27.986		

Complex **3**

	JTC (C_{3v})	JCCU (C_{4v})	CCU (C_{4v})	JCSAPR (C_{4v})	CSAPR (C_{4v})	JTCTPR (D_{3h})	TCTPR (D_{3h})
Dy(1)	14.974	10.414	8.287	2.128	1.461	2.414	1.199
	HP (D_{6h})	PPY (C_{5v})	OC (O_h)	TPR (D_{3h})	JPPY (C_{5v})		
Fe(1)	33.737	23.847	2.014	12.340	27.690		

JTC (C_{3v}): Johnson triangular cupola J3; JCCU (C_{4v}): Capped cube J8; CCU (C_{4v}): Spherical-relaxed capped cube; JCSAPR (C_{4v}): Capped square antiprism J10; CSAPR (C_{4v}): Spherical capped square antiprism; JTCTPR (D_{3h}): Tricapped trigonal prism J51; TCTPR (D_{3h}): Spherical tricapped trigonal prism; HP (D_{6h}): Hexagon; PPY (C_{5v}): Pentagonal pyramid; OC (O_h): Octahedron; TPR (D_{3h}): Trigonal prism; JPPY (C_{5v}): Johnson pentagonal pyramid J2.

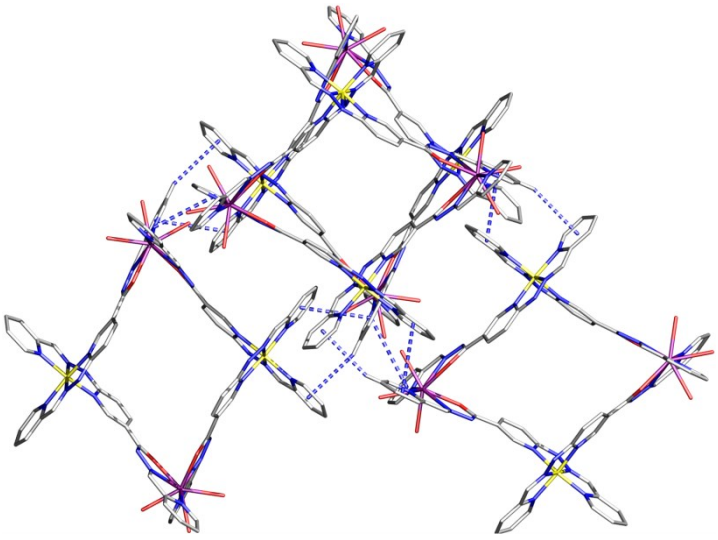

Figure S6. Illustration showing the π-π and C-H···π interactions in complex **1**.

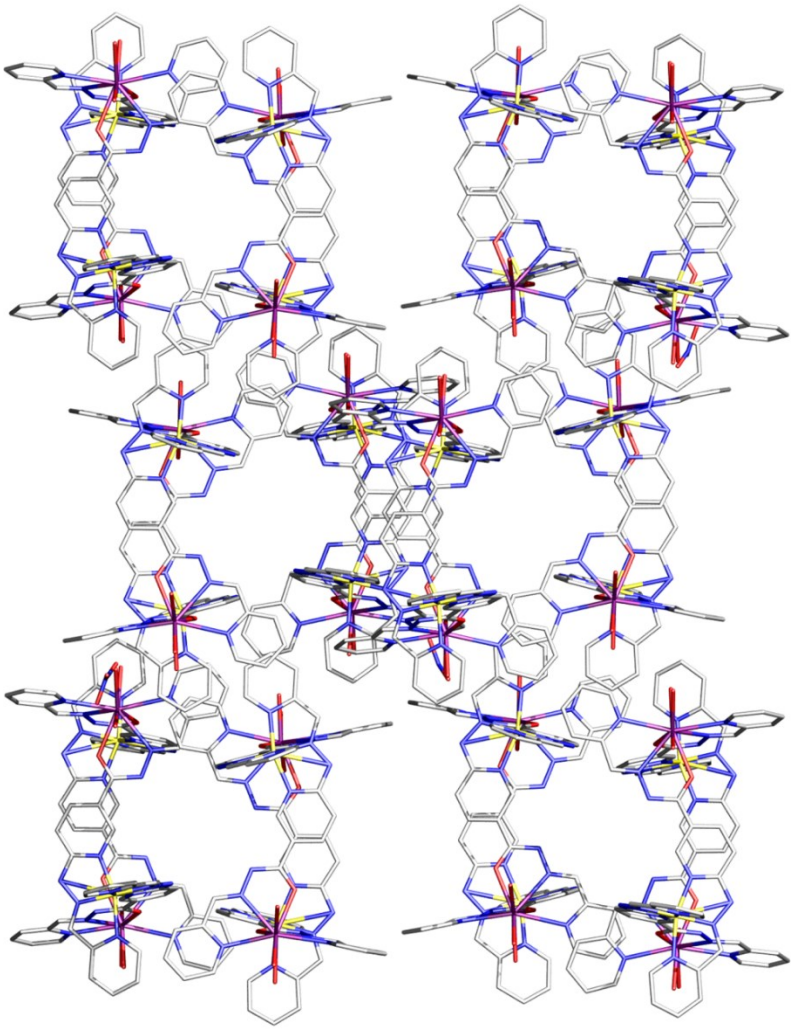

Figure S7. The crystal packing of complex **1**.

Table S4. Selected bond lengths (Å) for complex **2**.

Atom-Atom	Length/Å	Atom-Atom	Length/Å
Dy(1)-O(1)	2.387(5)	Dy(1)-N(1)	2.567(6)
Dy(1)-O(2)	2.407(5)	Dy(1)-N(2)	2.512(6)
Dy(1)-O(3)	2.432(5)	Dy(1)-N(12)	2.593(7)
Dy(1)-O(4)	2.373(6)	Dy(1)-N(13)	2.529(7)
Dy(1)-O(5)	2.343(6)		
Fe(1)-N(4)	1.992(6)	Fe(1)-N(8)	1.968(6)
Fe(1)-N(6)	1.866(6)	Fe(1)-N(10)	1.883(7)
Fe(1)-N(7)	1.947(5)	Fe(1)-N(11)	1.941(6)

Symmetry transformations used to generate equivalent atoms: #1 -x+1, -y+1/2, z+0

Table S5. Selected bond lengths (Å) for complex **2**.

Atom-Atom-Atom	Angle/°	Atom-Atom-Atom	Angle/°
O(5)-Dy(1)-O(4)	71.0(2)	O(2)-Dy(1)-N(13)	62.89(19)
O(5)-Dy(1)-O(1)	74.4(2)	O(3)-Dy(1)-N(13)	73.18(18)
O(4)-Dy(1)-O(1)	139.69(19)	N(2)-Dy(1)-N(13)	113.9(2)
O(5)-Dy(1)-O(2)	137.94(18)	O(5)-Dy(1)-N(1)	90.23(19)
O(4)-Dy(1)-O(2)	141.88(17)	O(4)-Dy(1)-N(1)	75.1(2)
O(1)-Dy(1)-O(2)	78.43(19)	O(1)-Dy(1)-N(1)	125.39(19)
O(5)-Dy(1)-O(3)	143.4(2)	O(2)-Dy(1)-N(1)	79.97(19)
O(4)-Dy(1)-O(3)	72.49(19)	O(3)-Dy(1)-N(1)	78.62(18)
O(1)-Dy(1)-O(3)	139.63(19)	N(2)-Dy(1)-N(1)	62.9(2)
O(2)-Dy(1)-O(3)	74.64(17)	N(13)-Dy(1)-N(1)	137.9(2)
O(5)-Dy(1)-N(2)	72.5(2)	O(5)-Dy(1)-N(12)	80.5(2)
O(4)-Dy(1)-N(2)	123.1(2)	O(4)-Dy(1)-N(12)	75.3(2)
O(1)-Dy(1)-N(2)	62.5(2)	O(1)-Dy(1)-N(12)	79.20(19)
O(2)-Dy(1)-N(2)	66.6(2)	O(2)-Dy(1)-N(12)	124.9(2)
O(3)-Dy(1)-N(2)	128.7(2)	O(3)-Dy(1)-N(12)	92.19(18)
O(5)-Dy(1)-N(13)	130.5(2)	N(2)-Dy(1)-N(12)	137.5(2)
O(4)-Dy(1)-N(13)	123.04(19)	N(13)-Dy(1)-N(12)	62.1(2)
O(1)-Dy(1)-N(13)	67.93(18)	N(1)-Dy(1)-N(12)	150.5(2)
N(6)-Fe(1)-N(10)	179.3(3)	N(11)-Fe(1)-N(8)	159.8(3)
N(6)-Fe(1)-N(11)	99.9(3)	N(7)-Fe(1)-N(8)	90.7(2)
N(10)-Fe(1)-N(11)	79.7(3)	N(6)-Fe(1)-N(4)	81.0(3)
N(6)-Fe(1)-N(7)	80.1(2)	N(10)-Fe(1)-N(4)	99.6(3)
N(10)-Fe(1)-N(7)	99.3(2)	N(11)-Fe(1)-N(4)	90.8(2)
N(11)-Fe(1)-N(7)	91.9(2)	N(7)-Fe(1)-N(4)	161.1(2)
N(6)-Fe(1)-N(8)	100.2(3)	N(8)-Fe(1)-N(4)	93.2(2)
N(10)-Fe(1)-N(8)	80.1(3)		

Symmetry transformations used to generate equivalent atoms: #1 -x+1, -y+1/2, z+0

Table S6. Selected bond lengths (Å) for complex **3**.

Atom-Atom	Length/Å	Atom-Atom	Length/Å
Dy(1)-O(1)	2.387(5)	Dy(1)-N(1)	2.586(4)
Dy(1)-O(2)	2.394(5)	Dy(1)-N(2)	2.519(7)
Dy(1)-O(3)	2.365(6)	Dy(1)-N(12)	2.606(7)
Dy(1)-O(4)	2.393(6)	Dy(1)-N(13)	2.539(7)
Dy(1)-O(5)	2.535(6)		
Fe(1)-N(4)	1.993(6)	Fe(1)-N(8)	1.962(4)
Fe(1)-N(6)	1.868(7)	Fe(1)-N(9)	1.895(6)
Fe(1)-N(7)	1.966(5)	Fe(1)-N(11)	1.966(5)

Symmetry transformations used to generate equivalent atoms: #1 -x+2, -y+3/2, z+0

Table S7. Selected bond lengths (Å) for complex **3**.

Atom-Atom-Atom	Angle/°	Atom-Atom-Atom	Angle/°
O(3)-Dy(1)-O(1)	74.7(2)	O(2)-Dy(1)-N(13)	62.27(19)
O(3)-Dy(1)-O(4)	70.7(2)	N(2)-Dy(1)-N(13)	114.2(2)
O(1)-Dy(1)-O(4)	139.2(2)	O(5)-Dy(1)-N(13)	72.45(19)
O(3)-Dy(1)-O(2)	138.04(19)	O(3)-Dy(1)-N(1)	88.74(19)
O(1)-Dy(1)-O(2)	78.01(19)	O(1)-Dy(1)-N(1)	125.26(16)
O(4)-Dy(1)-O(2)	142.75(18)	O(4)-Dy(1)-N(1)	75.25(17)
O(3)-Dy(1)-N(2)	72.0(2)	O(2)-Dy(1)-N(1)	81.59(16)
O(1)-Dy(1)-N(2)	62.71(19)	N(2)-Dy(1)-N(1)	62.56(18)
O(4)-Dy(1)-N(2)	123.1(2)	O(5)-Dy(1)-N(1)	79.79(15)
O(2)-Dy(1)-N(2)	67.3(2)	N(13)-Dy(1)-N(1)	139.07(19)
O(3)-Dy(1)-O(5)	144.4(2)	O(3)-Dy(1)-N(12)	80.3(2)
O(1)-Dy(1)-O(5)	138.52(19)	O(1)-Dy(1)-N(12)	78.48(19)
O(4)-Dy(1)-O(5)	73.8(2)	O(4)-Dy(1)-N(12)	75.0(2)
O(2)-Dy(1)-O(5)	73.69(16)	O(2)-Dy(1)-N(12)	124.5(2)
N(2)-Dy(1)-O(5)	128.39(19)	N(2)-Dy(1)-N(12)	136.7(2)
O(3)-Dy(1)-N(13)	130.8(2)	O(5)-Dy(1)-N(12)	93.18(18)
O(1)-Dy(1)-N(13)	67.7(2)	N(13)-Dy(1)-N(12)	62.3(2)
O(4)-Dy(1)-N(13)	122.7(2)	N(1)-Dy(1)-N(12)	150.21(19)
N(6)-Fe(1)-N(9)	179.5(3)	N(8)-Fe(1)-N(7)	92.1(2)
N(6)-Fe(1)-N(8)	99.1(2)	N(11)-Fe(1)-N(7)	90.5(2)
N(9)-Fe(1)-N(8)	80.5(2)	N(6)-Fe(1)-N(4)	80.9(2)
N(6)-Fe(1)-N(11)	100.4(3)	N(9)-Fe(1)-N(4)	99.4(3)
N(9)-Fe(1)-N(11)	80.0(3)	N(8)-Fe(1)-N(4)	89.8(2)
N(8)-Fe(1)-N(11)	160.5(2)	N(11)-Fe(1)-N(4)	94.1(2)
N(6)-Fe(1)-N(7)	79.6(2)	N(7)-Fe(1)-N(4)	160.5(2)
N(9)-Fe(1)-N(7)	100.1(2)		

Symmetry transformations used to generate equivalent atoms: #1 -x+2, -y+3/2, z+0

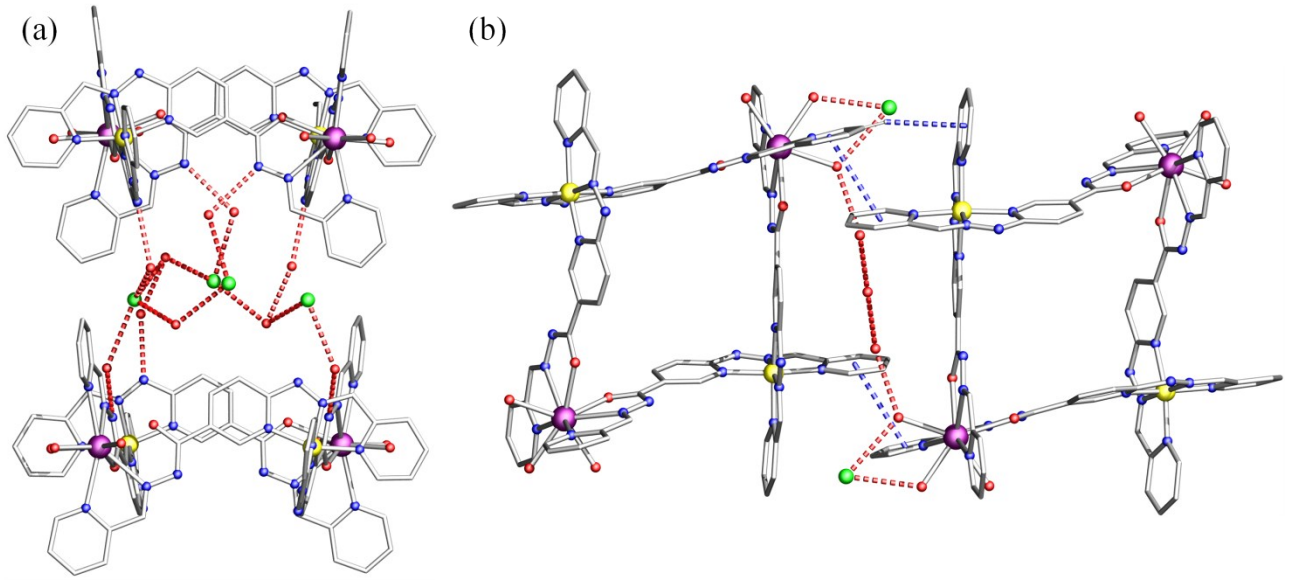

Figure S8. Illustration showing the hydrogen-bonding, π-π and C-H···π interactions in complex **2**.

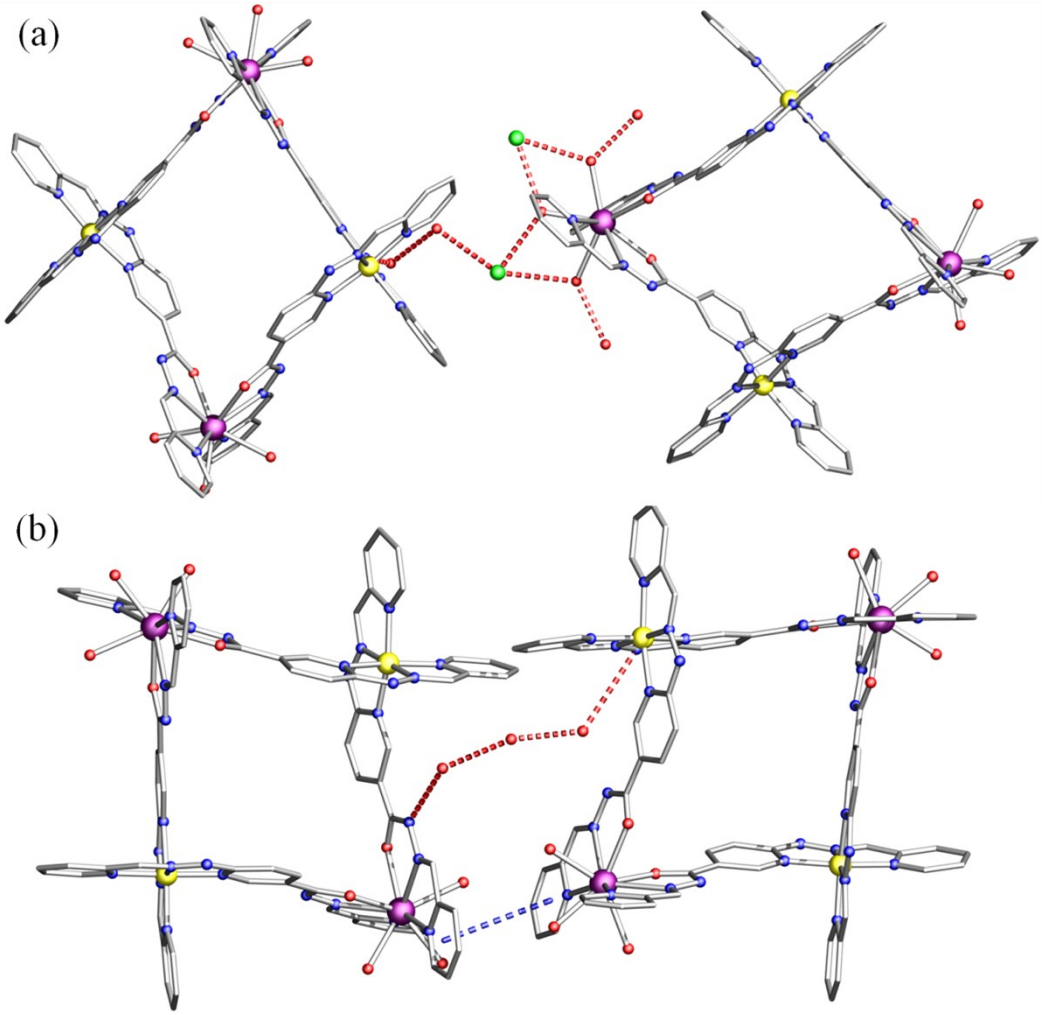

Figure S9. Illustration showing the hydrogen-bonding and π-π interactions in complex **3**.

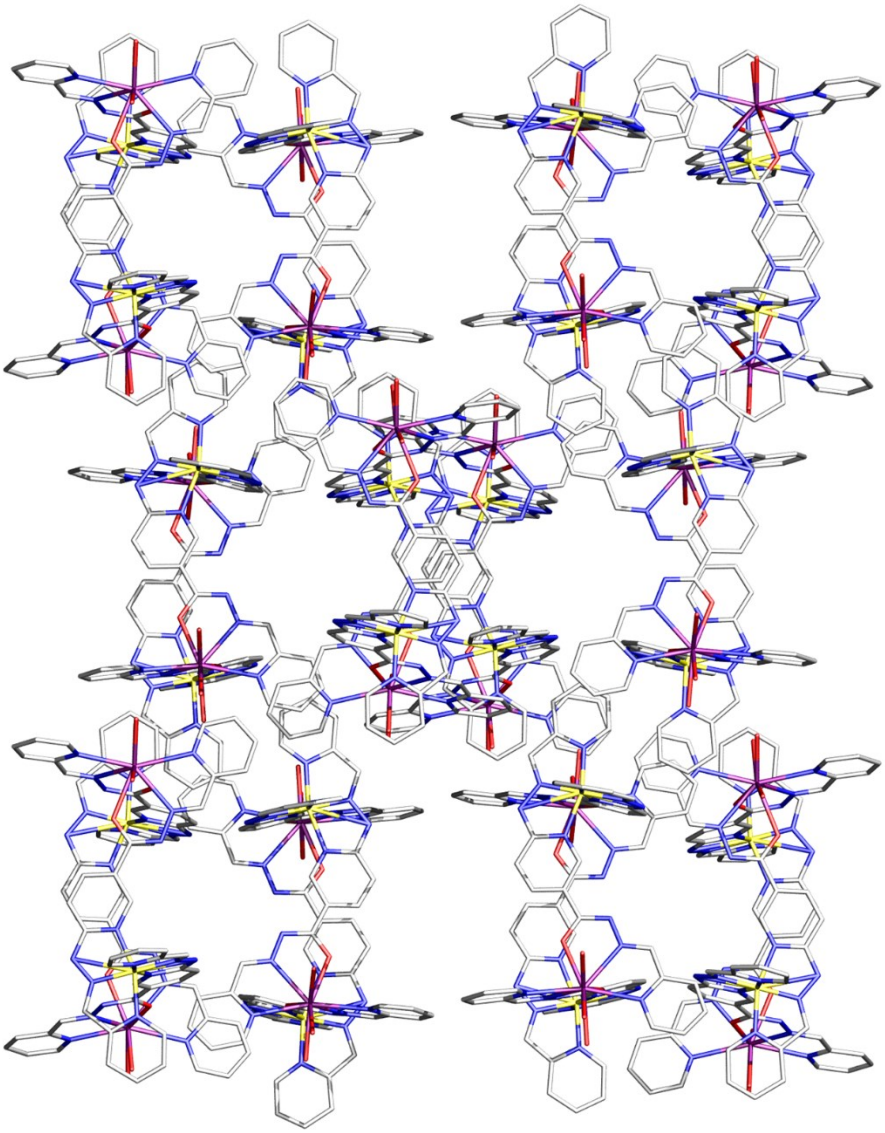

Figure S10. The crystal packing of complex **2**.

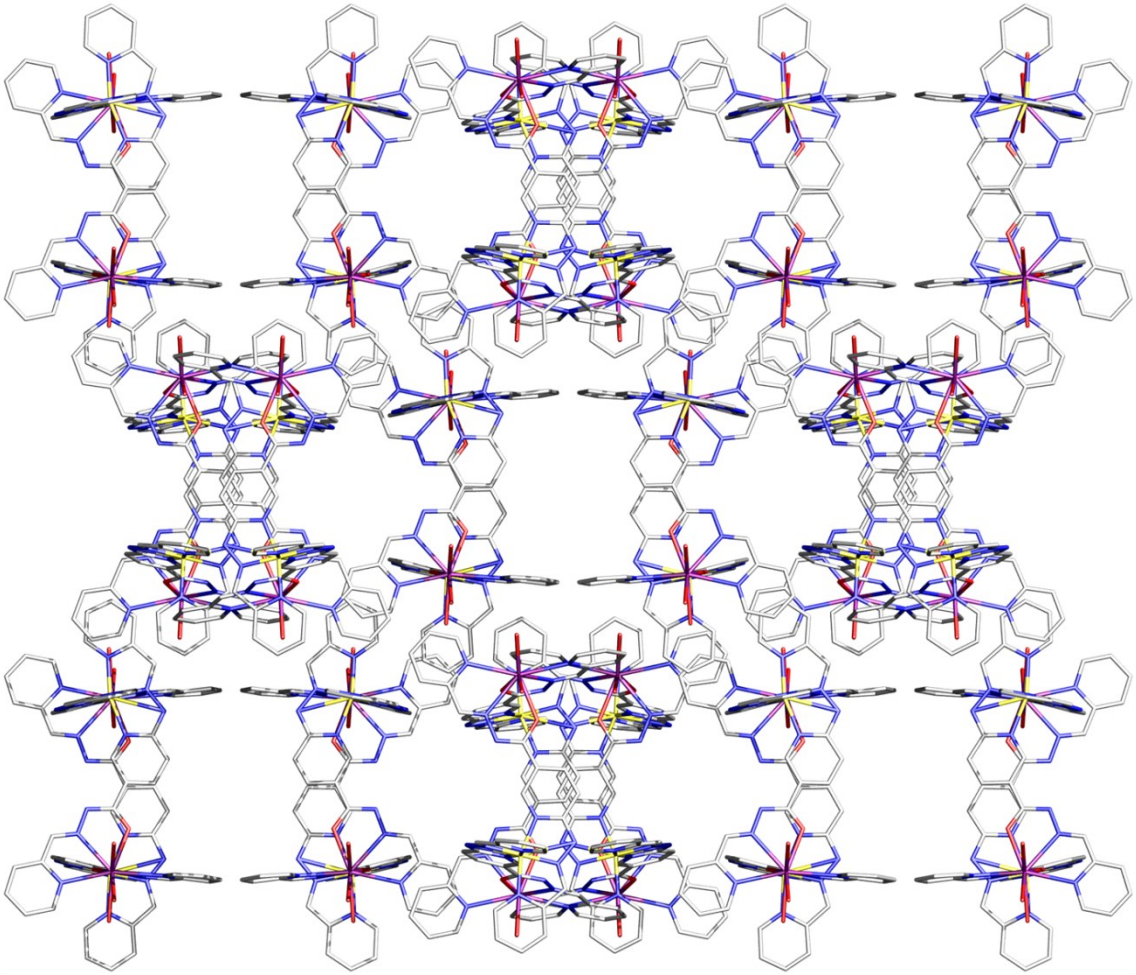

Figure S11. The crystal packing of complex **3**.

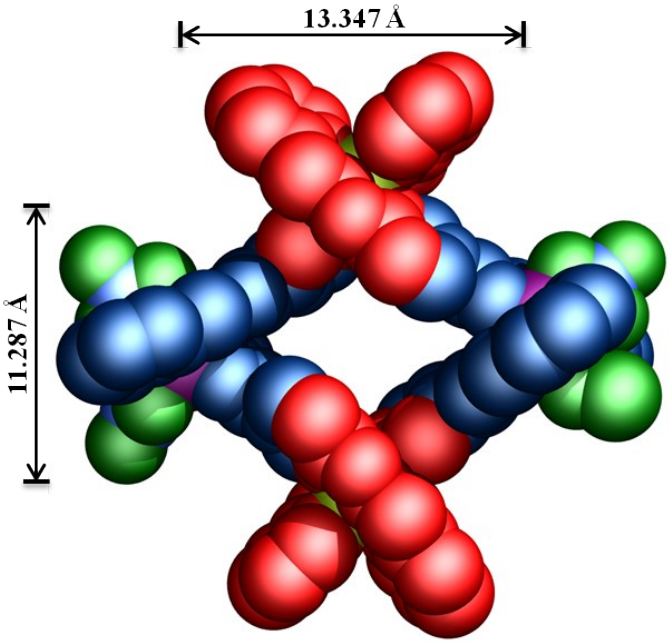

Figure S12. The Space-filling presentation of complex **4**.

Table S8. Selected bond lengths (Å) for complex **4**.

Atom-Atom	Length/Å	Atom-Atom	Length/Å
Dy(1)-O(3)	2.418(6)	Dy(2)-O(1)	2.360(6)
Dy(1)-O(4)	2.376(6)	Dy(2)-O(2)	2.321(6)
Dy(1)-O(9)	2.415(6)	Dy(2)-O(5)	2.484(7)
Dy(1)-O(10)	2.465(6)	Dy(2)-O(6)	2.446(7)
Dy(1)-O(12)	2.534(7)	Dy(2)-O(8)	2.349(6)
Dy(1)-O(13)	2.455(7)	Dy(2)-N(13)	2.517(8)
Dy(1)-N(1)	2.592(7)	Dy(2)-N(14)	2.569(9)
Dy(1)-N(2)	2.540(7)	Dy(2)-N(15)	2.544(8)
Dy(1)-N(27)	2.574(7)	Dy(2)-N(16)	2.487(7)
Dy(1)-N(28)	2.642(8)		
Fe(1)-N(4)	1.965(7)	Fe(2)-N(18)	1.981(7)
Fe(1)-N(6)	1.892(7)	Fe(2)-N(20)	1.872(7)
Fe(1)-N(7)	1.993(7)	Fe(2)-N(21)	1.984(8)
Fe(1)-N(8)	1.978(8)	Fe(2)-N(22)	1.979(8)
Fe(1)-N(9)	1.883(7)	Fe(2)-N(23)	1.836(7)
Fe(1)-N(11)	1.978(7)	Fe(2)-N(25)	1.953(7)

Table S9. Selected bond angles (°) for complex **4**.

Atom-Atom-Atom	Angle/°	Atom-Atom-Atom	Angle/°
O(4)-Dy(1)-O(9)	137.7(2)	O(12)-Dy(1)-N(28)	109.7(2)
O(4)-Dy(1)-O(3)	83.7(2)	N(2)-Dy(1)-N(28)	146.7(2)
O(9)-Dy(1)-O(3)	72.9(2)	N(27)-Dy(1)-N(28)	61.0(2)
O(4)-Dy(1)-O(13)	72.2(3)	N(1)-Dy(1)-N(28)	148.4(2)
O(9)-Dy(1)-O(13)	132.6(2)	O(2)-Dy(2)-O(8)	145.7(2)
O(3)-Dy(1)-O(13)	153.7(3)	O(2)-Dy(2)-O(1)	89.8(2)
O(4)-Dy(1)-O(10)	151.5(2)	O(8)-Dy(2)-O(1)	81.7(2)
O(9)-Dy(1)-O(10)	52.6(2)	O(2)-Dy(2)-O(6)	78.2(2)
O(3)-Dy(1)-O(10)	121.4(2)	O(8)-Dy(2)-O(6)	126.2(2)
O(13)-Dy(1)-O(10)	84.6(3)	O(1)-Dy(2)-O(6)	143.4(2)
O(4)-Dy(1)-O(12)	100.9(2)	O(2)-Dy(2)-O(5)	127.0(2)
O(9)-Dy(1)-O(12)	121.4(2)	O(8)-Dy(2)-O(5)	74.2(2)
O(3)-Dy(1)-O(12)	128.8(2)	O(1)-Dy(2)-O(5)	140.8(2)
O(13)-Dy(1)-O(12)	49.7(2)	O(6)-Dy(2)-O(5)	52.3(2)
O(10)-Dy(1)-O(12)	74.9(2)	O(2)-Dy(2)-N(16)	63.5(2)
O(4)-Dy(1)-N(2)	62.7(2)	O(8)-Dy(2)-N(16)	140.3(2)
O(9)-Dy(1)-N(2)	130.3(2)	O(1)-Dy(2)-N(16)	70.3(2)
O(3)-Dy(1)-N(2)	65.0(2)	O(6)-Dy(2)-N(16)	73.5(2)
O(13)-Dy(1)-N(2)	94.0(3)	O(5)-Dy(2)-N(16)	111.1(2)
O(10)-Dy(1)-N(2)	137.4(2)	O(2)-Dy(2)-N(13)	70.1(2)
O(12)-Dy(1)-N(2)	72.2(2)	O(8)-Dy(2)-N(13)	76.6(2)
O(4)-Dy(1)-N(27)	66.4(2)	O(1)-Dy(2)-N(13)	62.9(2)

O(9)-Dy(1)-N(27)	71.5(2)	O(6)-Dy(2)-N(13)	139.1(2)
O(3)-Dy(1)-N(27)	61.9(2)	O(5)-Dy(2)-N(13)	136.4(2)
O(13)-Dy(1)-N(27)	114.9(2)	N(16)-Dy(2)-N(13)	112.2(2)
O(10)-Dy(1)-N(27)	111.2(2)	O(2)-Dy(2)-N(15)	126.4(2)
O(12)-Dy(1)-N(27)	163.9(2)	O(8)-Dy(2)-N(15)	83.7(2)
N(2)-Dy(1)-N(27)	107.9(2)	O(1)-Dy(2)-N(15)	76.0(2)
O(4)-Dy(1)-N(1)	126.3(2)	O(6)-Dy(2)-N(15)	83.6(3)
O(9)-Dy(1)-N(1)	80.1(2)	O(5)-Dy(2)-N(15)	71.1(2)
O(3)-Dy(1)-N(1)	73.0(2)	N(16)-Dy(2)-N(15)	63.1(2)
O(13)-Dy(1)-N(1)	113.1(2)	N(13)-Dy(2)-N(15)	136.2(2)
O(10)-Dy(1)-N(1)	77.8(2)	O(2)-Dy(2)-N(14)	77.3(2)
O(12)-Dy(1)-N(1)	63.4(2)	O(8)-Dy(2)-N(14)	80.7(2)
N(2)-Dy(1)-N(1)	63.6(2)	O(1)-Dy(2)-N(14)	125.0(2)
N(27)-Dy(1)-N(1)	131.7(2)	O(6)-Dy(2)-N(14)	86.2(3)
O(4)-Dy(1)-N(28)	84.8(2)	O(5)-Dy(2)-N(14)	81.3(2)
O(9)-Dy(1)-N(28)	78.6(2)	N(16)-Dy(2)-N(14)	138.4(2)
O(3)-Dy(1)-N(28)	121.6(2)	N(13)-Dy(2)-N(14)	62.5(2)
O(13)-Dy(1)-N(28)	67.5(2)	N(15)-Dy(2)-N(14)	151.1(2)
O(10)-Dy(1)-N(28)	70.8(2)		
N(9)-Fe(1)-N(6)	179.3(3)	N(23)-Fe(2)-N(20)	178.5(3)
N(9)-Fe(1)-N(4)	98.4(3)	N(23)-Fe(2)-N(25)	82.2(3)
N(6)-Fe(1)-N(4)	82.0(3)	N(20)-Fe(2)-N(25)	98.7(3)
N(9)-Fe(1)-N(8)	80.4(3)	N(23)-Fe(2)-N(22)	80.4(3)
N(6)-Fe(1)-N(8)	100.1(3)	N(20)-Fe(2)-N(22)	98.8(3)
N(4)-Fe(1)-N(8)	92.5(3)	N(25)-Fe(2)-N(22)	162.5(3)
N(9)-Fe(1)-N(11)	81.8(3)	N(23)-Fe(2)-N(18)	100.2(3)
N(6)-Fe(1)-N(11)	97.6(3)	N(20)-Fe(2)-N(18)	81.0(3)
N(4)-Fe(1)-N(11)	90.3(3)	N(25)-Fe(2)-N(18)	91.1(3)
N(8)-Fe(1)-N(11)	162.2(3)	N(22)-Fe(2)-N(18)	90.6(3)
N(9)-Fe(1)-N(7)	99.4(3)	N(23)-Fe(2)-N(21)	98.3(3)
N(6)-Fe(1)-N(7)	80.2(3)	N(20)-Fe(2)-N(21)	80.6(3)
N(4)-Fe(1)-N(7)	162.1(3)	N(25)-Fe(2)-N(21)	90.6(3)
N(8)-Fe(1)-N(7)	89.3(3)	N(22)-Fe(2)-N(21)	93.3(3)
N(11)-Fe(1)-N(7)	93.4(3)	N(18)-Fe(2)-N(21)	161.5(3)

Table S10. Dy^{III} and Fe^{II} ions geometry analysis of complex **4** by SHAPE 2.1 software.[4-7]

	JBCCU (D_{4h})	JBCSAPR (D_{4d})	JMBIC (C_{2v})	JATDI (C_{3v})	JSPC (C_{2v})	SDD (D_2)	TD (D_{2v})
Dy(1)	11.446	4.621	8.207	16.878	2.985	4.669	3.889
	JTC (C_{3v})	JCCU (C_{4v})	CCU (C_{4v})	JCSAPR (C_{4v})	CSAPR (C_{4v})	JTCTPR (D_{3h})	TCTPR (D_{3h})
Dy(2)	13.785	10.179	9.134	3.027	1.717	2.846	2.209
	HP (D_{6h})	PPY (C_{5v})	OC (O_h)	TPR (D_{3h})	JPPY (C_{5v})		
Fe(1)	33.140	23.942	1.707	12.418	27.814		
Fe(2)	33.811	24.124	1.769	12.209	28.044		

JBCCU (D_{4h}): Bicapped cube J15; JBCSAPR (D_{4d}): Bicapped square antiprism J17; JMBIC (C_{2v}): Metabidiminished icosahedron J62; JATDI (C_{3v}): Augmented tridiminished icosahedron J64; JSPC-10(C_{2v}): Sphenocorona J87; SDD (D_2): Staggered Dodecahedron (2:6:2); TD (D_{2v}): Tetradecahedron (2:6:2); JTC (C_{3v}): Johnson triangular cupola J3; JCCU (C_{4v}): Capped cube J8; CCU (C_{4v}): Spherical-relaxed capped cube; JCSAPR (C_{4v}): Capped square antiprism J10; CSAPR (C_{4v}): Spherical capped square antiprism; JTCTPR (D_{3h}): Tricapped trigonal prism J51; TCTPR (D_{3h}): Spherical tricapped trigonal prism; HP (D_{6h}): Hexagon; PPY (C_{5v}): Pentagonal pyramid; OC (O_h): Octahedron; TPR (D_{3h}): Trigonal prism; JPPY (C_{5v}): Johnson pentagonal pyramid J2.

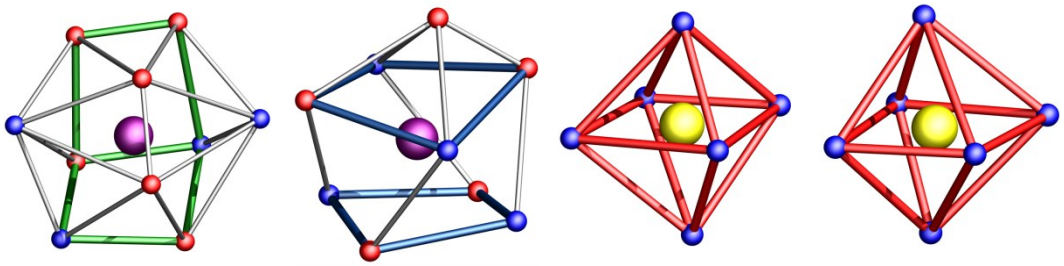

Figure S13. Coordination polyhedra observed in complex **4**: sphenocorona for Dy1 (green), spherical tricapped trigonal prism for Dy2 (blue) and octahedral environment for Fe1 and Fe2 (red), respectively.

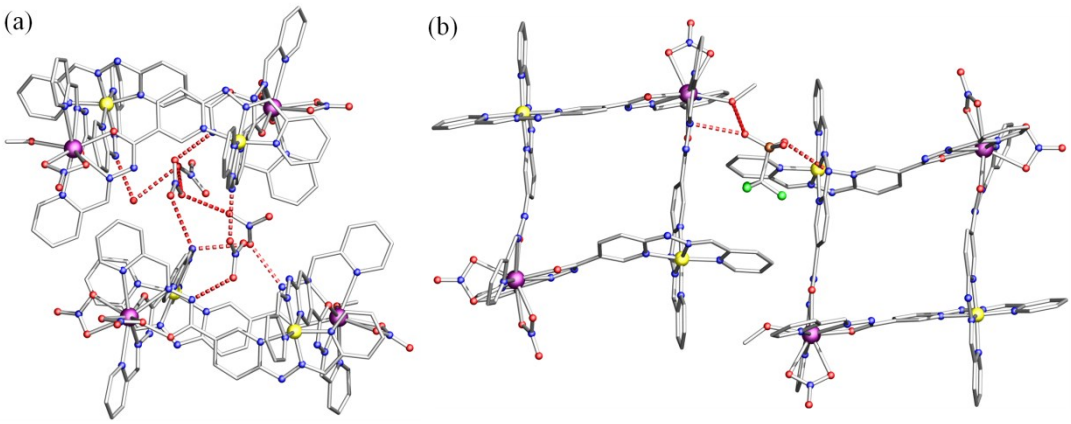

Figure S14. Illustration showing the hydrogen-bonding interactions in complex **4**.

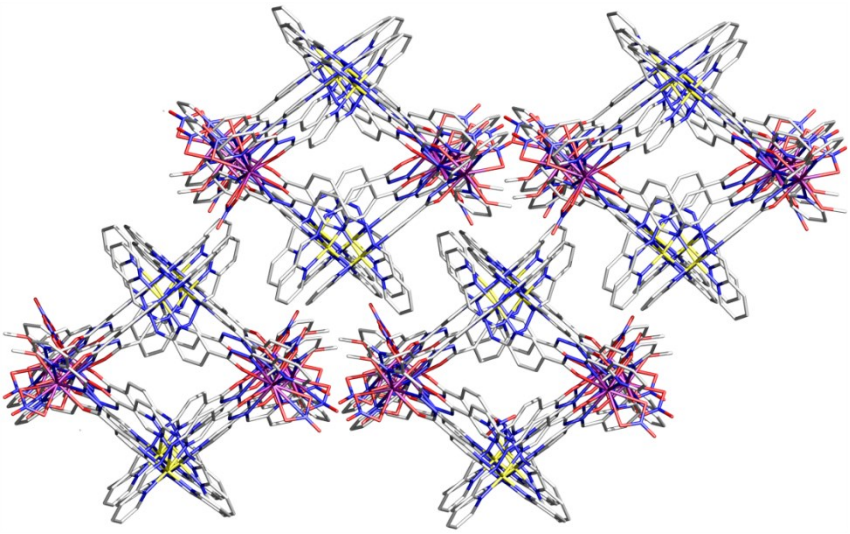

Figure S15. The crystal packing of complex **4**.

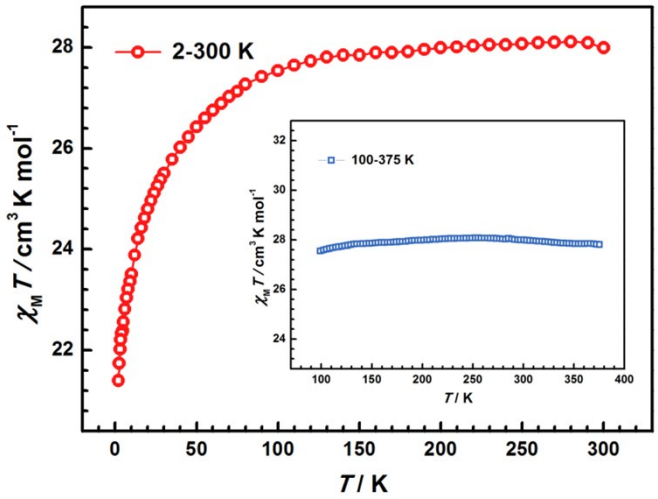

Figure S16. Plots of $\chi_M T$ vs T for complex **1**.

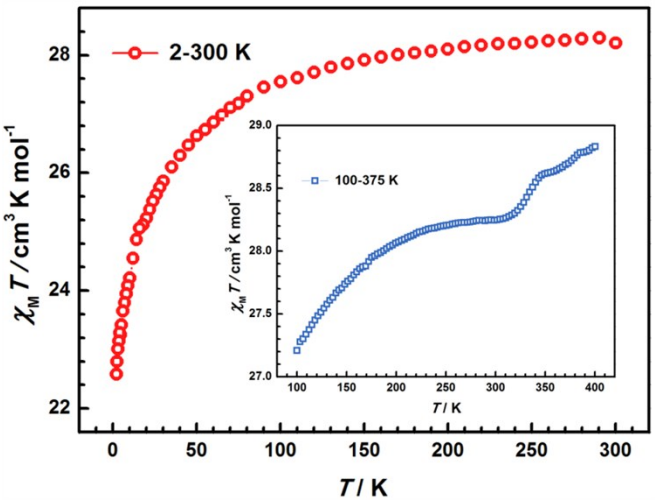

Figure S17. Plots of $\chi_M T$ vs T for complex **3**.

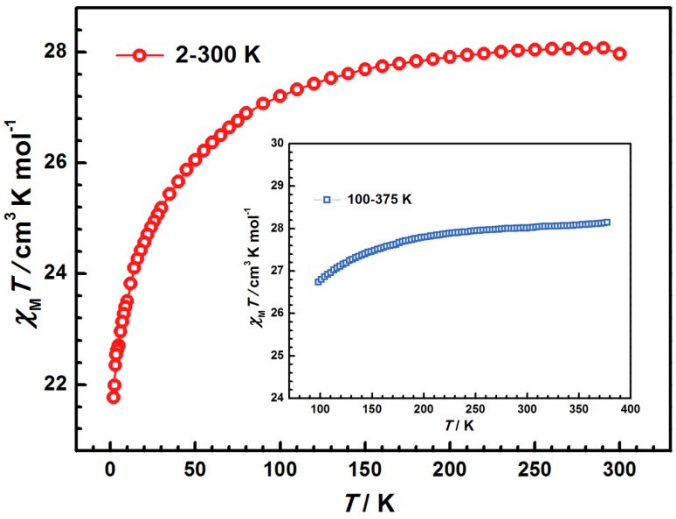

Figure S18. Plots of $\chi_M T$ vs T for complex **4**.

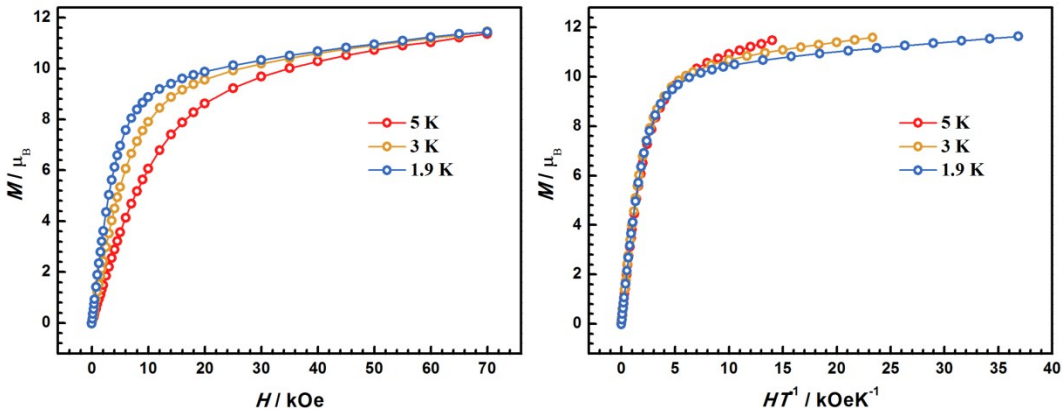

Figure S19. Molar magnetization (M) versus magnetic field (H) for complex **1** (left). Plots of the reduced magnetization M versus H/T (right).

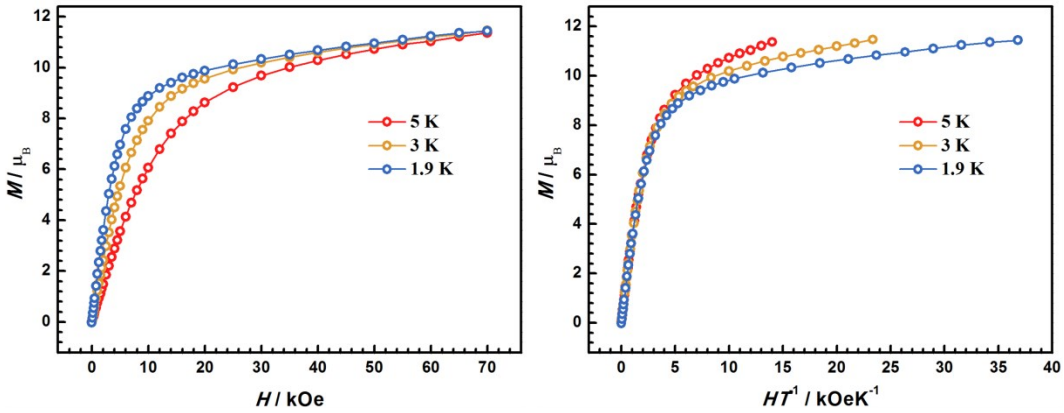

Figure S20. Molar magnetization (M) versus magnetic field (H) for complex **2** (left). Plots of the reduced magnetization M versus H/T (right).

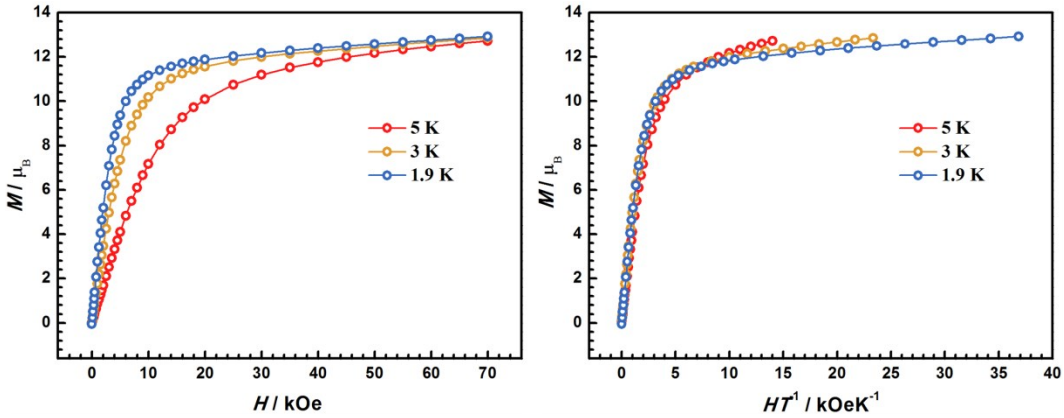

Figure S21. Molar magnetization (*M*) versus magnetic field (*H*) for complex **3** (left). Plots of the reduced magnetization *M* versus *H*/*T* (right).

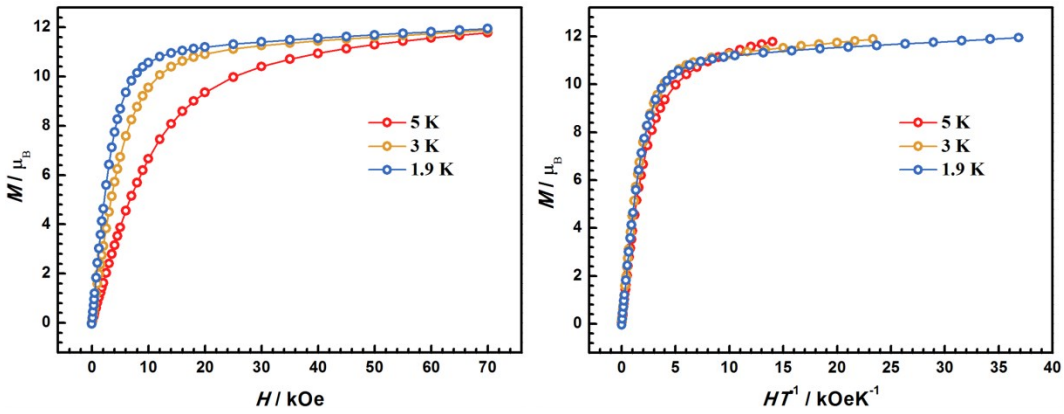

Figure S22. Molar magnetization (*M*) versus magnetic field (*H*) for complex **4** (left). Plots of the reduced magnetization *M* versus *H*/*T* (right).

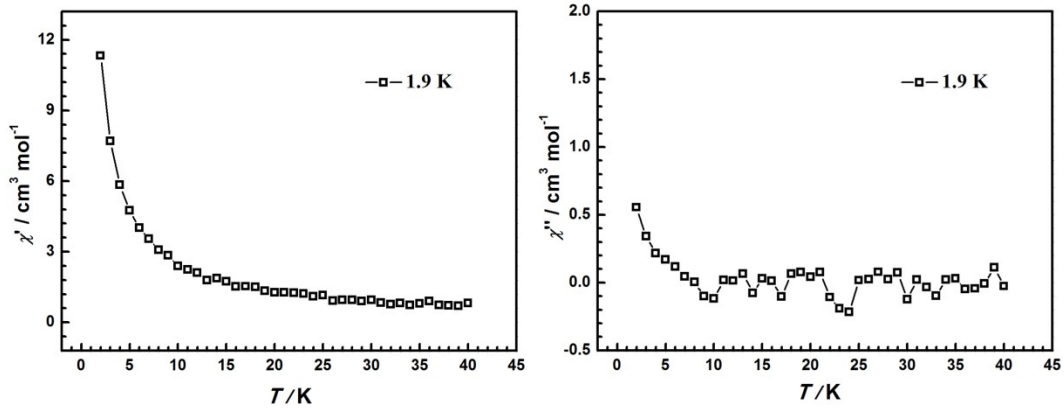

Figure S23. Temperature-dependence in-phase (left) and out-of-phase (right) susceptibility of complex **1** under a 0 Oe dc field.

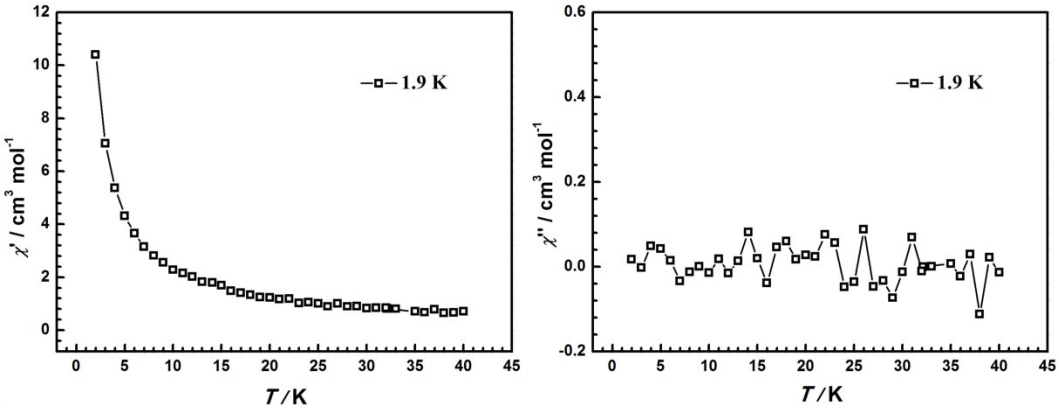

Figure S24. Temperature-dependence in-phase (left) and out-of-phase (right) susceptibility of complex **2** under a 0 Oe dc field.

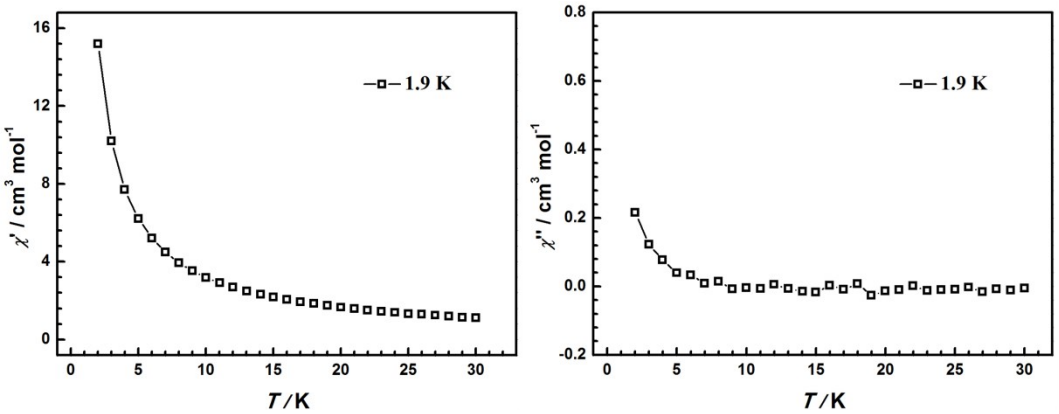

Figure S25. Temperature-dependence in-phase (left) and out-of-phase (right) susceptibility of complex **3** under a 0 Oe dc field.

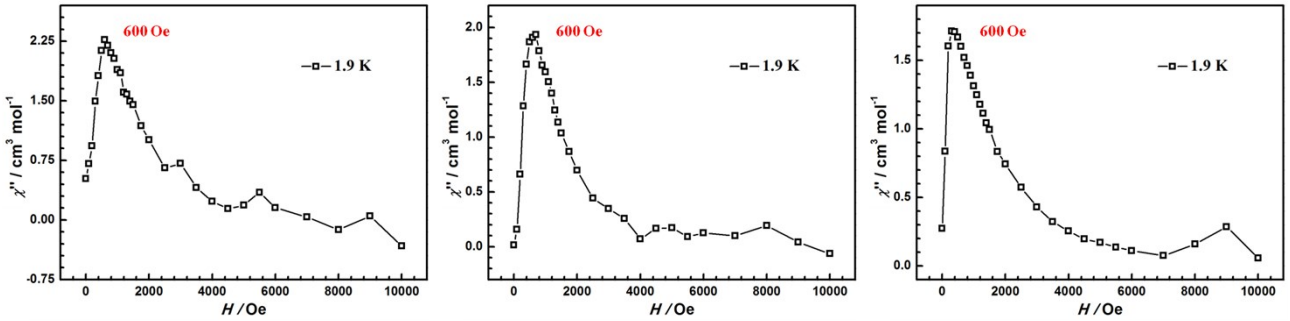

Figure S26. The field dependence of the out-of-phase signals of complexes **1-3** on applied dc field strength at 1.9 K, 997 Hz.

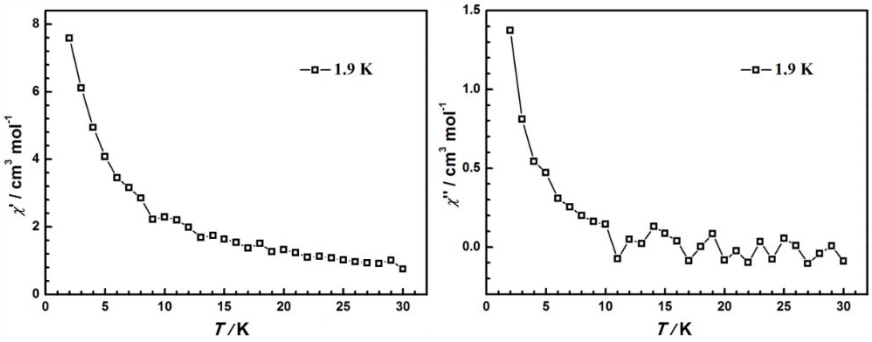

Figure S27. Temperature-dependence in-phase (left) and out-of-phase (right) susceptibility of complex **1** under a 600 Oe dc field.

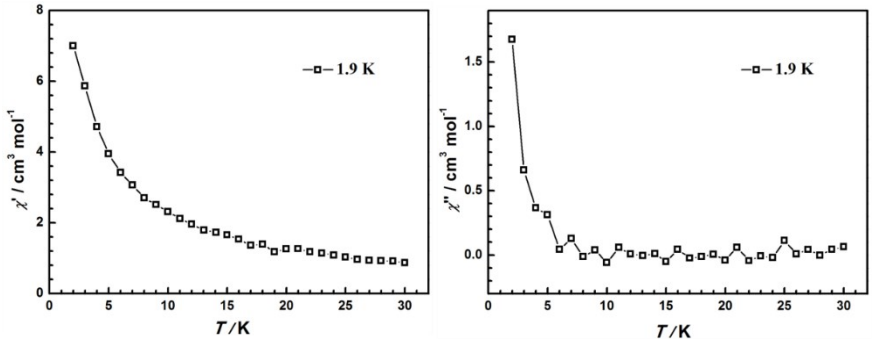

Figure S28. Temperature-dependence in-phase (left) and out-of-phase (right) susceptibility of complex **2** under a 600 Oe dc field.

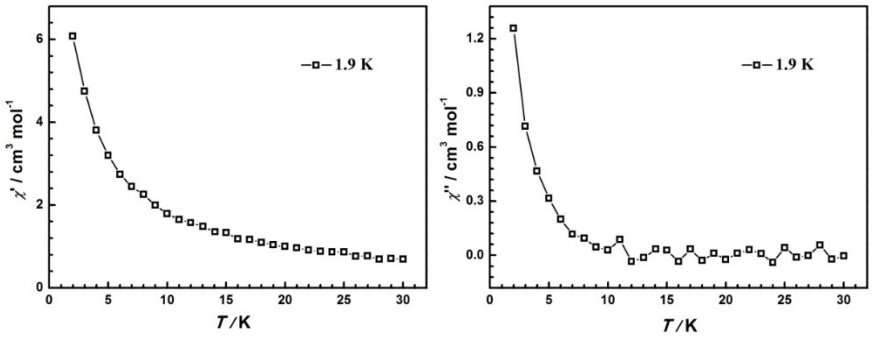

Figure S29. Temperature-dependence in-phase (left) and out-of-phase (right) susceptibility of complex **3** under a 600 Oe dc field.

Reference

(1) Bain, G. A.; Berry, J. F. *J. Chem. Educ.* **2008**, *85*, 532.
(2) Sheldrick, G. *Acta Crystallogr. Sect. A: Found. Adv.* **2015**, *71*, 3.
(3) Sheldrick, G. *Acta Crystallogr. Sect. C: Struct. Chem.* **2015**, *71*, 3.
(4) Alvarez, S.; Avnir, D.; Llunell, M.; Pinsky, M. *New J. Chem.* **2002**, *26*, 996.
(5) Alvarez, S.; Alemany, P.; Casanova, D.; Cirera, J.; Llunell, M.; Avnir, D. *Coord. Chem. Rev.* **2005**, *249*, 1693.
(6) Ruiz-Martínez, A.; Casanova, D.; Alvarez, S. *Chem. – Eur. J.* **2008**, *14*, 1291.
(7) Ruiz-Martínez, A.; Alvarez, S. *Chem. – Eur. J.* **2009**, *15*, 7470.